Transmission-Phase Relations of Four-Frequency Parametric Devices*

D. B. ANDERSON†, MEMBER, IRE, AND J. C. AUKLAND†, MEMBER, IRE

Summary—The gain, bandwidth, and excess noise temperature properties of parametric amplifiers are generally known. However, a knowledge of their transmission-phase properties is also essential for the effective application of parametric amplifiers to angular detection systems, such as monopulse radars and interferometers. These angle detection systems derive even, odd, and quadrupolar spatial components of the antenna diffraction patterns. The differential amplitude and differential phase between these signal components contain the spatial information of position, extent, and shape of the target. Consequently, to employ parametric transducers in certain systems requires an understanding of the transmission phase properties which are delineated in this paper.

The analysis follows the matrix representation of a nonlinear capacitive susceptance, four-frequency transducer wherein due note is taken of the phases. The transmission-phase relations are written which include the effects of nonzero port susceptance and nonlinear reactance element losses. At midband without losses, the relations reduce to easily remembered equations which are significant to the application of parametric transducers in phase-sensitive systems. Some applications and experimental results are cited.

I. Introduction

LOW-NOISE parametric amplification is now a reality, and its application to receiver systems is being seriously considered. The gain, bandwidth, and excess noise temperature properties of parametric amplifiers are generally known. However, a knowledge of the transmission-phase property of parametric amplifiers is also essential to their effective application in certain types of phase-sensitive systems. The transmission-phase relations are the phase shifts associated with the transmission coefficient of the transition between the various ports of a transducer.[1]

For example, a monopulse angle-detection radar employs an antenna and a hybrid-junction labyrinth which derives even, odd, and quadrupolar spatial components of the antenna diffraction pattern. The source signal or target echo differential amplitude and differential phase between labyrinth ports contain spatial information of target position, extent, and shape.[2] Consequently, to employ parametric transducers for low-noise amplification, or to implement the phase-detection function in monopulse systems, requires a knowledge of their transmission-phase properties.

The gain, bandwidth, and noise properties for the various operational modes of four-frequency parametric devices have been considered previously.[3–8]

The authors' intent is to delineate the transmission-phase properties of four-frequency parametric devices.

The signal phases in each permitted port are interrelated through the pump phase by the mixing process which occurs in the nonlinear element. Four-frequency parametric transducers (signal, pump, upper sideband, and lower sideband) are considered because they encompass both the negative conductance and the frequency conversion mechanisms of amplification which individually appear in the three-frequency difference and sum spectral modes, respectively. As the signal frequencies in the three-frequency difference mode converge to the two-frequency degenerate mode, the amplification of the single unique frequency (one-half the pump frequency) is sensitive to the relative pump phase. The four-frequency transmission-phase relations will be developed; from these the relations for three- and two-frequency devices are obvious.

In this report the method of analysis uses the well-known matrix representation for a nonlinear capacitive-susceptance four-frequency parametric transducer wherein due note is taken of the phases. A lossy nonlinear reactive element and the effects of nonzero port susceptances are considered, removing the midband restrictions on the transmission-phase relations written previously.[9] Use of the transmission-phase relations will be illustrated by their application to several non-

* Received by the PGMTT, May 16, 1961; revised manuscript received, July 31, 1961.

† Autonetics Div., N. American Aviation, Inc., Anaheim, Calif.

[1] "IRE Standards on Antennas and Waveguides," PROC. IRE, vol. 47, pp. 568–582; April, 1959.

[2] D. B. Anderson and D. R. Wells, "Some Further Notes on the Spatial Information available from Monopulse Radar," presented at 5th MIL-E-CON Natl. Convention on Military Electronics, Washington, D. C.; June 26–28, 1961.

[3] E. M. T. Jones and J. S. Honda, "A low-noise up-converter parametric amplifier," 1959 IRE WESCON CONVENTION RECORD, pt. 1, pp. 99–107.

[4] D. K. Adams, "An analysis of four-frequency nonlinear reactance circuits," IRE TRANS. ON MICROWAVE THEORY AND TECHNIQUES, vol. MTT-8, pp. 274–283; May, 1960.

[5] D. B. Anderson and J. C. Aukland, "A general catalog of gain, bandwidth, and noise temperature expressions for four-frequency parametric devices," submitted for publication, IRE TRANS. ON MICROWAVE THEORY AND TECHNIQUES.

[6] C. Blake, "Review of Reactance Amplifier Circuit Theory," Lincon Lab., Mass. Inst. Tech., Lexington, Rept. No. 46G-004; July 7, 1960.

[7] C. R. Boyd, "A general approach to the evaluation of *n*-frequency parametric mixers," *Proc. NEC*, vol. 16, pp. 472–479; October, 1960.

[8] J. A. Luksch, E. Q. Matthews, and G. A. VerWys, "Design and operation of four-frequency parametric up-converters," IRE TRANS. ON MICROWAVE THEORY AND TECHNIQUES, vol. MTT-9, pp. 44–52; January, 1961.

[9] D. B. Anderson and J. C. Aukland, "The midband phase relations in four-frequency parametric amplifiers," Symp. on the Application of Low-Noise Receivers to Radar and Allied Equipment, Lincoln Lab., October 24–28, 1960; Mass. Inst. Tech., Lexington, vol. 3, pp. 165–175; November 22, 1960.

reciprocal and unilateral parametric transducers. A discussion follows of some wideband transmission-phase-measurement techniques and their experimental results for several operational modes. The transmission-phase relations developed should not be confused with the interrelations of propagation constants that have been defined for travelling wave structures.

II. Development of Transmission-Phase Relations

In the following cursory analysis the four-frequency parametric transducer considered is represented by Fig. 1.

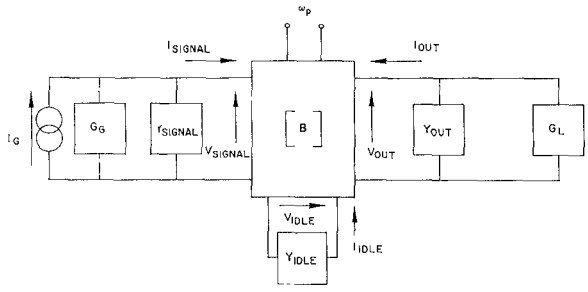

Fig. 1—General four-frequency parametric transducer.

For small signal conditions, the current components in the time-varying susceptance are represented in matrix notation as

$$[I_n] = [B][V_n] \tag{1}$$

for each port at frequency ω_n, where the nonlinear susceptance is represented by the admittance matrix $[B]$, and the current and the voltage at each port are described by matrices $[I_n]$ and $[V_n]$, respectively. The capacitive susceptance realized in a back-biased semiconductor diode is considered because of its general acceptance for low-noise applications. A single large periodic pump voltage $V_p(t)$ causes the capacitance to vary as

$$C[V_p(t)] = C_0 + \frac{C_1}{2} + \frac{C_1^*}{2}$$

$$= C_0 + |C_1|e^{j(\omega_p t+\phi_p)} + |C_1|^* e^{-j(\omega_p t+\phi_p)}. \tag{2}$$

The asterisk (*) denotes C_1^* as the conjugate of C_1, where C_0 is the capacitance due to the fixed bias, and C_1 is the time variation of capacitance about C_0 caused by the pumping voltage $V_p(t)$.

In the microwave region the back-biased semiconductor diode only approaches the ideal nonlinear capacity because the spreading resistance R_s is in series with the barrier capacity. Using the admittance representation of the diode, the equivalent conductance is written as

$$G_{dn} = \frac{\omega_n^2 C_0^2 R_s}{1 + \omega_n^2 C_0^2 R_s^2}, \tag{3}$$

and the equivalent capacitive susceptance is written as

$$B_{dn} = \frac{\omega_n C_0}{1 + \omega_n^2 C_0^2 R_s^2} \tag{4}$$

at the ports $n=1, 2, 3$. Practical microwave varactors have a high Q where the diode Q at each frequency ω_n is

$$Q_{dn} = \frac{1}{\omega_n C_0 R_s}, \tag{5}$$

so that a simplification of the equivalent conductance and susceptance is valid, and (3) and (4) become

$$G_{dn} = \omega_n^2 C_0^2 R_s \tag{6}$$

and

$$B_{dn} = \omega_n C_0. \tag{7}$$

The nomenclature for the four-frequencies which shall be allowed to exist in the external ports will be described as

$$\omega_1 < \omega_2 = \omega_p - \omega_1 < \omega_p < \omega_3 = \omega_p + \omega_1. \tag{8}$$

There are certain frequencies greater than ω_3 which are generated by the nonlinear reactance, but power at these frequencies is not permitted to exist in the external ports. The matrix equation (1), when written for the four frequencies specified in (8), where the effective diode loss at each frequency ω_n from (6) has been included in the diagonal term, is

$$\begin{bmatrix} I_1 \\ I_2^* \\ I_3 \end{bmatrix} = \begin{bmatrix} \omega_1^2 C_0^2 R_s + j\omega_1 C_0 & j\frac{\omega_1 C_1}{2} & j\frac{\omega_1 C_1^*}{2} \\ -j\frac{\omega_2 C_1^*}{2} & \omega_2^2 C_0^2 R_s - j\omega_2 C_0 & 0 \\ j\frac{\omega_3 C_1}{2} & 0 & \omega_3^2 C_0^2 R_s + j\omega_3 C_0 \end{bmatrix} \begin{bmatrix} V_1 \\ V_2^* \\ V_3 \end{bmatrix}. \tag{9}$$

The preceding equation fully describes the mixing process that occurs in the nonlinear element. The Kirchhoff current equations for each port of the nonlinear reactance, neglecting the generator current, are written as

$$I_1 = -V_1Y_1 = -V_1(G_1 - jB_1) \tag{10}$$

$$I_2^* = -V_2^*Y_2 = -V_2^*(G_2 + jB_2) \tag{11}$$

$$I_3 = -V_3Y_3 = -V_3(G_3 - jB_3), \tag{12}$$

where $(G_n \pm jB_n)$ represents the Y_n admittance associated with each port for which the susceptance term B_n cancels the diode susceptance $\omega_n C_0$ at the midband frequency line $\omega_n = \omega_{n0}$ of the mode spectrum.

The transmission-phase relations may now be determined where the phase dependencies of the voltage in (9)–(12) are included. As an example, consider a four-frequency operational mode spectrum with the input at ω_1, the output at ω_2, and the idle at ω_3. The output current from (9) is given by

$$I_2^* = (\omega_2^2 C_0^2 R_s - j\omega_2 C_0)V_2^* - j\frac{\omega_2 C_1^*}{2}V_1, \tag{13}$$

which will be equated to (11). Collecting real and imaginary terms after including the pump dependency of (2), the expression has the form of

$$K_r e^{j(\omega_2 t+\phi_2)} + K_i e^{j(\omega_2 t+\phi_2+\pi/2)} = K_t e^{j(\omega_2 t+\phi_p-\phi_1-\pi/2)}, \tag{14}$$

where ϕ_n is the phase of the voltage V_n, and the phasor magnitudes are given as

$$K_r = (G_2 + \omega_2^2 C_0^2 R_s)V_2 \tag{15}$$

$$K_i = (\omega_2 C_0 - B_2)V_2 \tag{16}$$

$$K_t = \frac{\omega_2 C_1}{2}V_1. \tag{17}$$

Eq. (14) has a graphical interpretation as phasors in Fig. 2.

Inspection of Fig. 2 readily yields the transmission phase at the output due to the signal input and the pumping of the nonlinear reactance as

$$\phi_2 = \phi_p - \phi_1 - \frac{\pi}{2} - \tan^{-1}\left(\frac{K_i}{K_r}\right). \tag{18}$$

Defining $\omega_n = \omega_{n0}(1+\delta_n)$ for each port, where ω_{n0} is the midband resonant frequency of the external port, and δ_n is the fractional deviation from resonance, (18) becomes

$$\phi_2 = \phi_p - \phi_1 - \frac{\pi}{2} - \tan^{-1}\left\{\frac{\omega_{20}^2 L_2 C_0(1+\delta_2)^2 - 1}{L_2 G_2 \omega_{20}(1+\delta_2)\left[1 + \dfrac{\omega_{20}^2(1+\delta_2)^2 C_0^2 R_S}{G_2}\right]}\right\}, \tag{19}$$

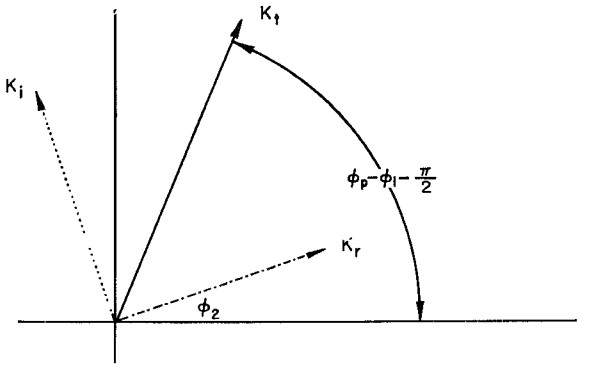

Fig. 2—Graphical interpretation of transmission phase.

where the external susceptance B_n has been assumed to be $1/\omega_n L_n$. For simple resonant cavities where its $Q = 1/\omega_n L_n G_n$, (19) becomes

$$\phi_2 = \phi_p - \phi_1 - \frac{\pi}{2} - \tan^{-1}\left[\frac{2Q_2\delta_2}{1 + \dfrac{1}{Q_{d2}^2 G_2 R_S}}\right], \tag{20}$$

where $\delta_n \ll 1$.

The arctangent term in (20) accounts for the varactor losses and detuning or off-center frequency operation of the output cavity. The constant $\pi/2$ in the phase relation (20) is reminiscent of the phase shift in a quarter-wave transformer. It should be noted that the phase of the input voltage in (20) is that at the input port or the nonlinear reactance and may not be the signal voltage phase applied to an input lossy cavity. The additional transmission phase shift through the input passive cavity may be accounted for in the conventional manner.

Now consider a four-frequency operational mode spectrum, where the input is at ω_1, the output is at ω_3, and the idle at ω_2; an argument analogous to the previous case yields the relation

$$\phi_3 = \phi_p + \phi_1 - \frac{\pi}{2} - \tan^{-1}\left[\frac{2Q_3\delta_3}{1 + \dfrac{1}{Q_{d1} G_3 R_S}}\right], \tag{21}$$

where $\delta_n \ll 1$.

The results of (20) and (21) are distinguished by the difference in sign of ϕ_1.

Now consider the four-frequency operational mode, where the input is at ω_2, the output is at ω_1, and the idle is at ω_3.

$$I_1 = (\omega_1^2 C_0^2 R_s + j\omega_1 C_0)V_1 + j\frac{\omega_1 C_1}{2}V_2^* + j\frac{\omega_1 C_1^*}{2}V_3, \tag{22}$$

which is equated to (10). From (9) and (12) V_3 is written in terms of V_1 and collecting the terms as before yields the relation

$$\phi_1 = \phi_p - \phi_2 - \frac{\pi}{2} - \tan^{-1}\left[\frac{\dfrac{2Q_1\delta_1}{1+\dfrac{1}{Q_{d1}{}^2R_sG_1}} - \dfrac{2a_{31}Q_3\delta_3}{1+\dfrac{1}{Q_{d3}{}^2R_sG_3}}}{1+a_{31}}\right], \quad (23)$$

where $\delta_n \ll 1$

$$a_{31} = \frac{\omega_1\omega_3 |C_1|^2}{4(G_1+\omega_1{}^2C_0{}^2R_s)(G_3+\omega_3{}^2C_0{}^2R_s)}. \quad (24)$$

The parameter a_{mn} is a measure of the coupling from the ω_m to ω_n port due to a pumping of a nonlinear reactance.

Similarly, for the four-frequency operational mode with the input at ω_3, the output at ω_1, and the idle at ω_2, the transmission-phase relation is

$$\phi_1 = \phi_3 - \phi_p - \frac{\pi}{2} - \tan^{-1}\left[\frac{\dfrac{2Q_1\delta_1}{1+\dfrac{1}{Q_{d1}G_1R_s}} - \dfrac{2a_{21}Q_2\delta_2}{1+\dfrac{1}{Q_{d2}{}^2G_2R_s}}}{1-a_{21}}\right], \quad (25)$$

where $\delta_n \ll 1$

$$a_{21} = \frac{\omega_1\omega_2 |C_1|^2}{4(G_1+\omega_1{}^2C_0{}^2R_s)(G_2+\omega_2{}^2C_0{}^2R_s)}. \quad (26)$$

Note that the form of (23) and (25) is similar, except that in (25) the pump and signal phase terms are interchanged. This is to be expected since the role of ω_p and ω_3 in the down-conversion mechanism from the sum frequency ω_3 acts like the difference-frequency mechanism, insofar as energy transfer is concerned. In both (23) and (25) the parametric coupling parameter a_{mn} shows how the idle cavity influences the transmission-phase properties.

Now, with the transmission-phase relations between ports of different frequencies (20), (21), (23), and (25), the phase properties of one-port parametric transducers (employing ferrite circulators to separate input and output ports at a single frequency) may be deduced by noting the transmission-phase conversion into the idle loading, then by noting the reflection at the idle port, and then by writing these in the transmission phase relation back to the original port.

The arctangent term of (20), (21), (23), and (25) expresses the effect of cavity detuning in the external ports and the diode losses on the phase. Note that at midband $\delta_n = 0$ the varactor loss does not influence the phase. The midband transmission-phase relations are more useful in the cursory analysis of phase-sensitive instrumentation, so by inspection the midband relations for various operational modes are tabulated as

Input to Output	Phase Relation	
$\omega_1 \rightarrow \omega_2$	$\phi_2 = \phi_p - \phi_1 - \frac{\pi}{2}$	(27)
$\omega_1 \rightarrow \omega_3$	$\phi_3 = \phi_p + \phi_1 - \frac{\pi}{2}$	(28)
$\omega_2 \rightarrow \omega_1$	$\phi_1 = \phi_p - \phi_2 - \frac{\pi}{2}$	(29)
$\omega_3 \rightarrow \omega_1$	$\phi_1 = \phi_3 - \phi_p - \frac{\pi}{2}$	(30)
$\omega_2 \rightarrow \omega_3$	$\phi_3 = 2\phi_p - \phi_2 - \pi$	(31)
$\omega_3 \rightarrow \omega_2$	$\phi_2 = 2\phi_p - \phi_3.$	(32)

The four-output transmission-phase relations (27)–(30) are easily remembered by noting the symmetry whereby the phases combine in the same manner as the frequencies combine, the result being in quadrature with the output phase, where the quadrature sign is determined by the nonlinear reactance. From these four basic relations, a simple manipulation yields (31) and (32) for conversion between the pump sidebands. These six equations may be applied for any type of nonlinear mixing elements by using the appropriate radian constant —negative constants for capacitive, positive constants for inductive, and no constants for resistive nonlinear elements.

The transmission-phase relations are also valid for the three-frequency case, wherein one of the pump side-bands is made nonexistent by setting $G_{\text{idle}} = \infty$ so $a_{mn} = 0$. A three-frequency difference transducer, wherein ω_1 and ω_2 are both coupled to the same port, is said to be degenerate, because, for the single unique frequency (one-half the pump $\phi_1 = \phi_2$) and from (29), the pump phase is

$$\phi_p = 2\phi_1 + \frac{\pi}{2} \quad (33)$$

to realize amplification.

III. Some Applications of Transmission-Phase Relations

Phase-sensitive systems measure the differential phase between the signals received in separate channels. Parametric devices used to amplify or process the signals must preserve the phase coherence between the channels. This requirement dictates the following:

1) A single-pump oscillator must be common to all channels.
2) Like parametric operation, modes must be used to preserve the signal-spectrum order.
3) The signal-selectivity bandwidth and transmission-line (signal and pump) electrical length must be similar for each channel to prevent signal dispersion.

When parametric devices are used in monopulse systems, the transmission-phase relations have proven use-

ful in system analysis in the same manner as the transmission phase rules have distinguished difference between the various microwave hybrid-junction types used in the design of monopulse labyrinths. The phase relations may also be used to conceive nonreciprocal or unilateral parametric devices. Some applications will be illustrated by applying the phase relations to two parametric devices described in the literature. The block diagram and mode spectrum of a nonreciprocal device[10] is illustrated in Fig. 3.

This device employs an up-converter followed by a down-converter, both pumped from a common source but in phase quadrature. From (28) and (30) the phase at each point for each direction of propagation is indicated in Fig. 3. It is clear that the device's phase length depends upon the direction of propagation because of the manner in which the pump is applied. Thus, when surrounded with two hybrid junctions, the device functions as a four-port circulator.

Adams[4] and Blake[6] have described a five-frequency parametric amplifier which has positive input-output conductances, unlimited conversion gain, and may be unilateral. The pump harmonic is employed as the fifth frequency. The principles which they employ combine two operational modes. If the modes are separated into individual parametric transducers of equal gain between two hybrid junctions and pumped coherently, then a four-port circulator is obtained, as illustrated in Fig. 4.

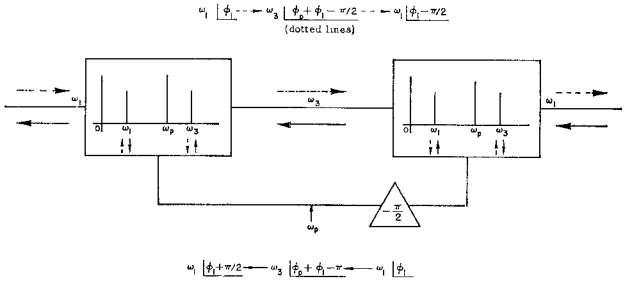

Fig. 3—A parametric nonreciprocal transducer.

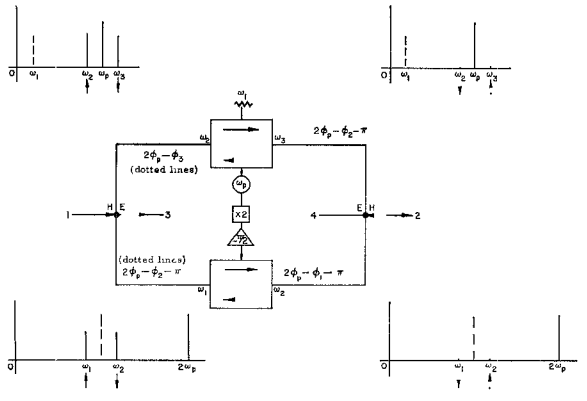

Fig. 4—A parametric 4-port circulator.

One amplifier functions in the three-frequency mode with respect to the ω_{2p} pump, where ω_{2p} is the second harmonic of ω_p. The other amplifier functions as a four-frequency device with respect to the ω_p pump, where ω_1 idles. From (27), (29), (30), and (32), the phase at each port for each direction of propagation is illustrated in Fig. 4. The frequencies on the opposite sides of the circulator are related as $\omega_2=\omega_1'$ and $\omega_3=\omega_2'$, where the primes signify the frequencies from the device pumped by ω_{2p}. It is clear that the signal will circulate as $1\rightarrow2\rightarrow3\rightarrow4\rightarrow1$, where both the signal frequencies and signal levels alternate between ports.

IV. Experimental Phase Measurements

Several experiments have been performed to verify some of the stated transmission-phase relations and to determine the application feasibility of parametric transducers in phase-sensitive instrumentation such as monopulse systems. The block diagram of instrumentation used to simultaneously measure the transmission gain and phase of a parametric amplifier over a wide frequency band is illustrated in Fig. 5. The frequencies in each leg of the phase bridge are separated by 1000 cps, and the total length of each leg is approximately 1700 wavelengths. The phase measurements are independent of signal amplitude over a 30-db dynamic range. Provisions are also included to measure the effective input noise temperature. A three-frequency difference parametric amplifier, operating in a quasi-degenerate mode with a pump of 17.0 Gc was used for the phase experiments. The parametric amplifier was designed for flexibility rather than wideband and low-noise temperature, although a 1.9 Gc gain-bandwidth product and 110°K radiometric noise temperature have been observed. The amplifier was designed to study the quasi-degenerate four-frequency operation and to accept a wide variety of varactor diodes with self-resonant frequencies both above and below the degenerate point.

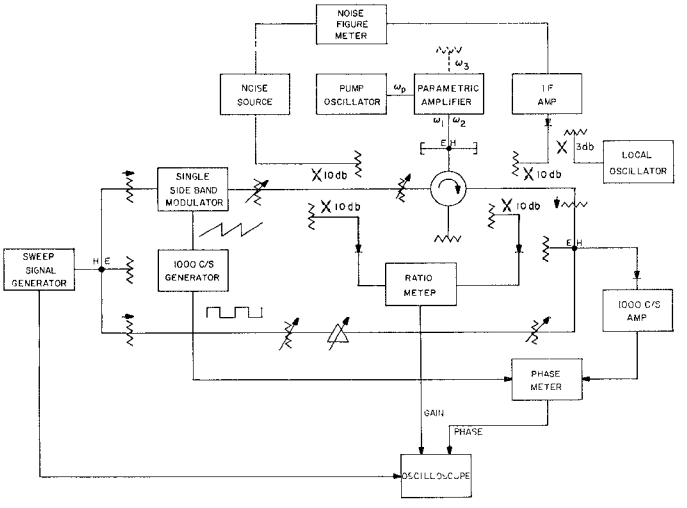

Fig. 5—Gain and phase instrumentation.

[10] A. K. Kamal, "A parametric device as a nonreciprocal element," Proc. IRE, vol. 48, pp. 1424–1430; August, 1960.

The observed experimental transmission gain and phase properties for a variety of operating conditions are illustrated in Figs. 6–11 (pp. 496–498). Relative power gain and differential phase 0 to 2π is displayed as a function of frequency for the conditions indicated.

Some explanation of the phase data displayed is prudent here for proper interpretation. A phase function is a continuous circular function which has been recorded herein on a rectilinear system; therefore, when the phase meter and oscillogram indicators reach 0 or 2π, the indicator rapidly traverses the scale and continues the phase function. The transmission-phase data of a degenerate parametric amplifier is shown in Fig. 6 for 0 and π positions of the phase shifter in the opposite leg of the phase bridge. Both curves are identical phase functions, but the upper curve has the scale traversal positioned at the amplifier midband.

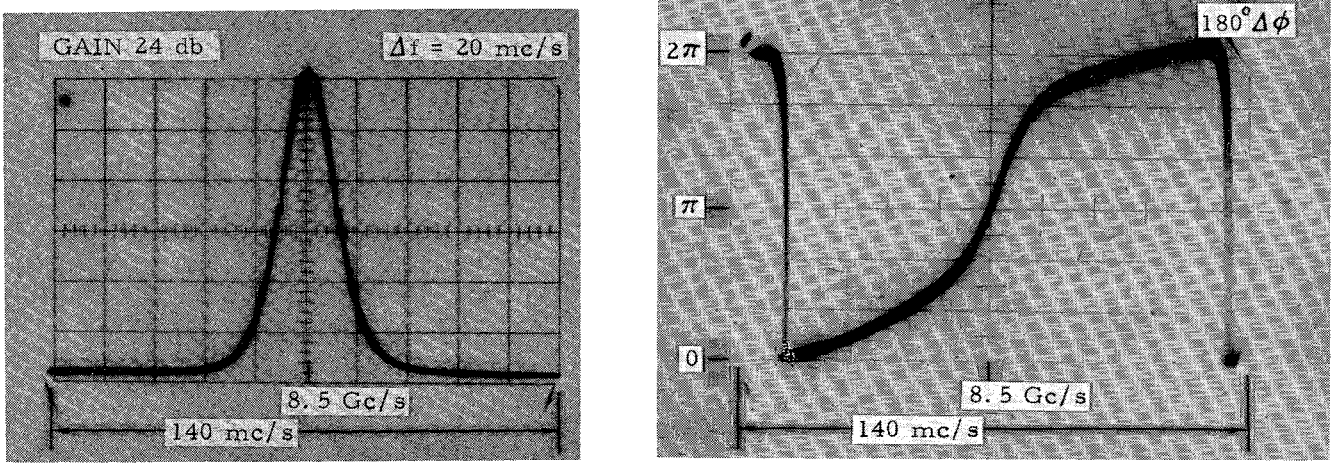

(a) (b)

Fig. 6—Transmission gain and phase as a function of frequency for a degenerate parametric amplifier. (a) Gain. (b) Phase

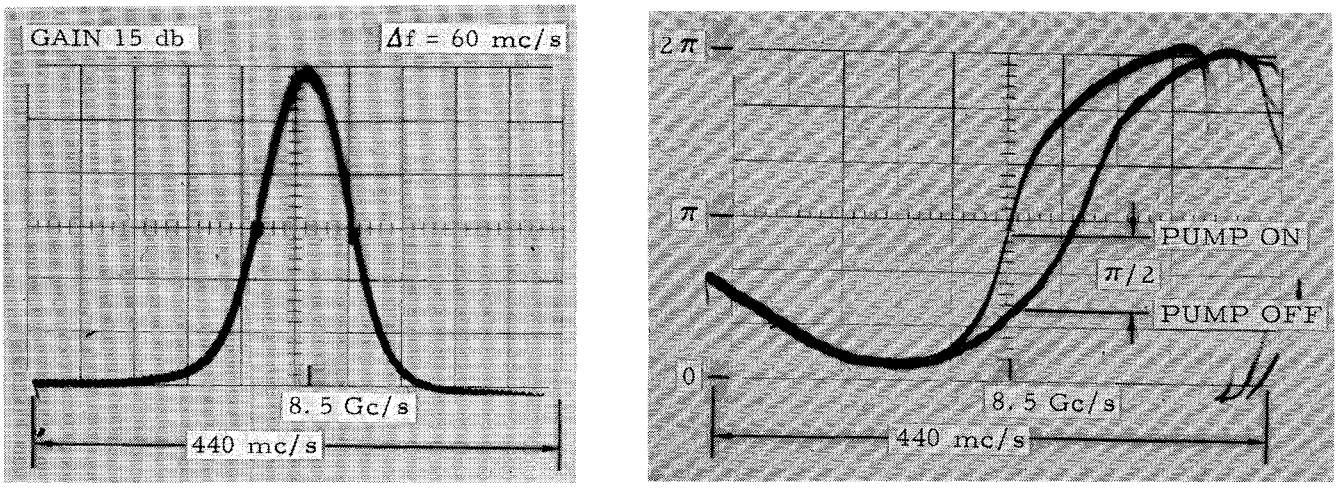

(a) (b)

Fig. 7—Transmission gain and phase as a function of frequency for a degenerate parametric amplifier, pump on and pump off. (a) Gain. (b) Phase.

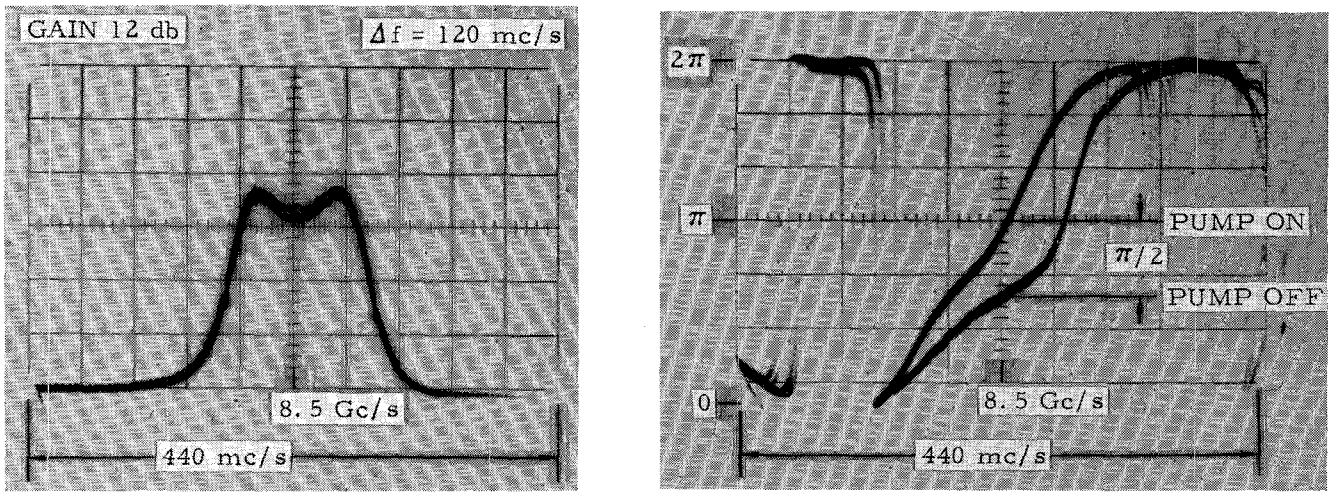

(a) (b)

Fig. 8—Transmission gain and phase as a function of frequency for a wideband degenerate parametric amplifier, pump on and pump off. (a) Gain. (b) Phase.

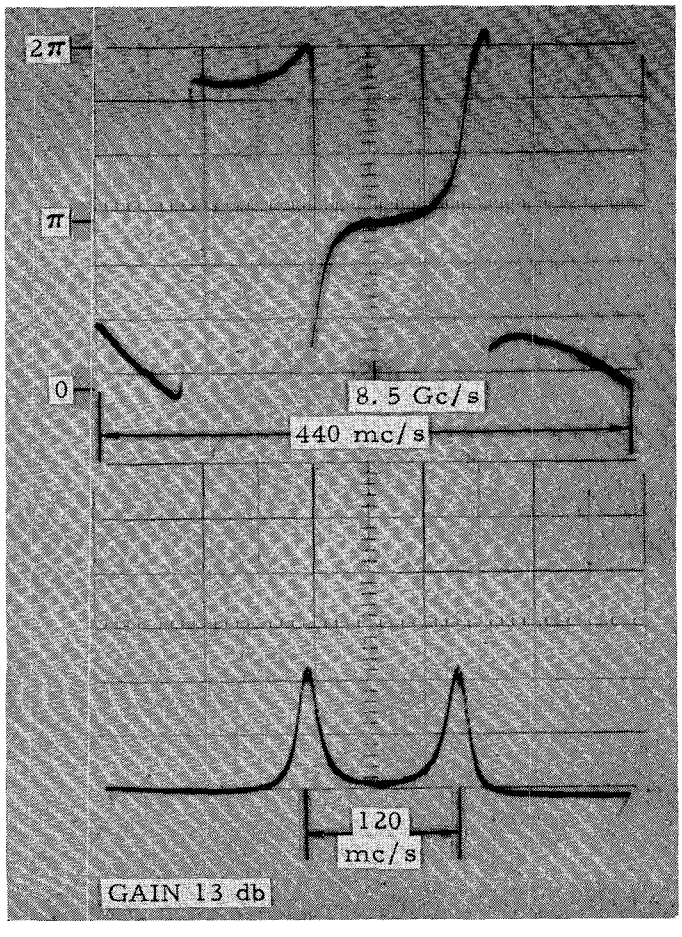

Fig. 9—Transmission gain and phase as a function of frequency for a nondegenerate parametric amplifier.

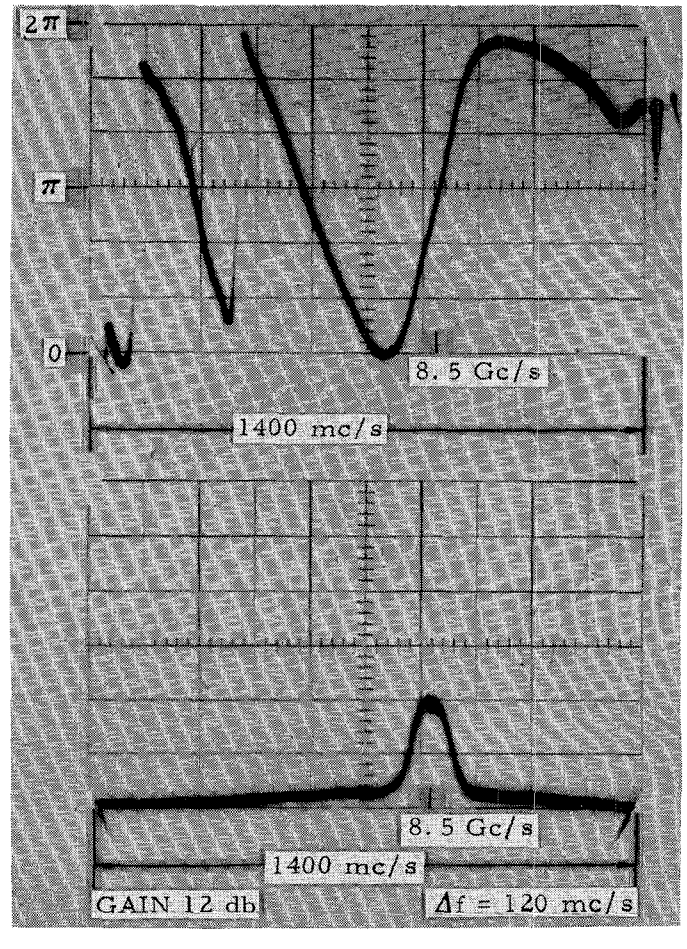

Fig. 10—Transmission gain and phase as a function of frequency of a wideband parametric amplifier showing the phase bridge dispersion properties over a wide band.

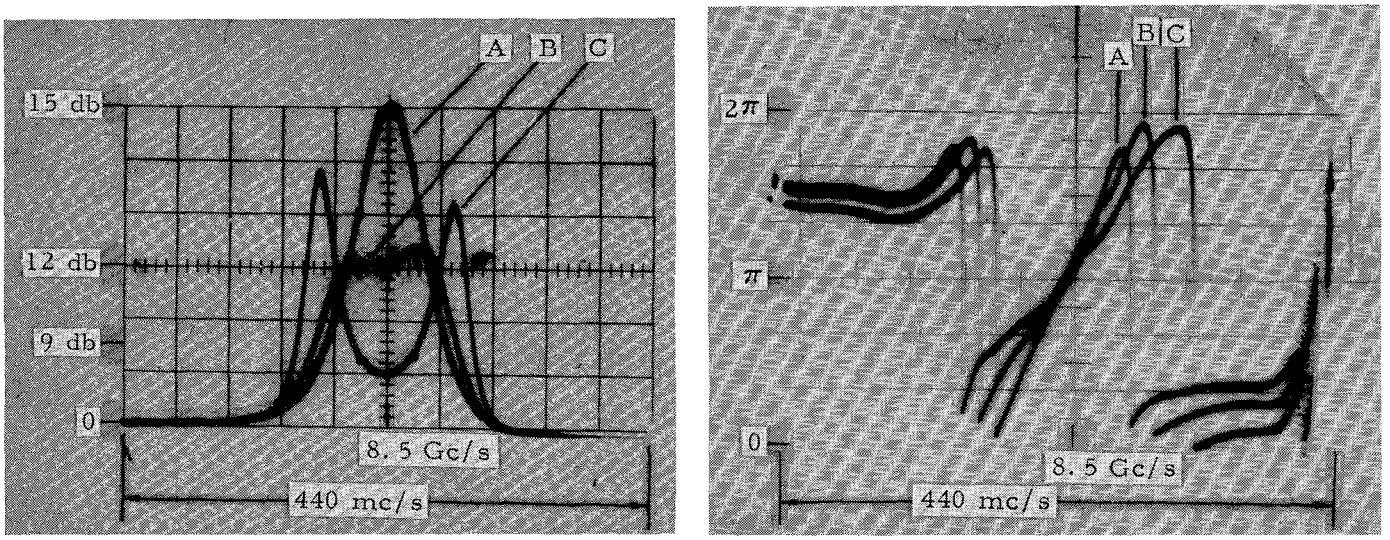

(a) (b)

Fig. 11—Transmission gain and phase as a function of frequency for three conditions of input coupling. (a) Gain. (b) Phase.

In Figs. 7 and 8 the upper phase curve is associated with the functioning amplifier, while the lower phase curve is for the transducer's cavity response without pump power. Note the $\pi/2$ shift at midband, which is to be expected from (27) and (29). The amplifier gain response in Fig. 8 for approximate critical coupling between ω_1 and ω_2 circuits is shown again in Fig. 10 with a sweep display width of 1.4 Gc. The two left scale traversals show the dispersion in the phase bridge which is the result of only crude compensation of coaxial components and helix in the TWT single sideband modulator. In Fig. 9 the amplifier shows separate responses for ω_1 and ω_2, and the corresponding phase curve unfortunately has the scale traversals aligned with the amplifier response. The gain and phase response for three successive degrees of coupling are shown in Fig. 11 in which the phases remain unchanged at $\delta_n = 0$. Similar results are observed when the ω_3 loading is altered.

The short-time stability of the phase-measuring system shown in Fig. 5 was observed to be less than one degree. No particular effort was made to stabilize the pump frequency, the signal frequency, or the TWT frequency translator.

When the conditions for coherent phase measurements are fulfilled in a monopulse receiver, the unpredictable variations of the differential phase stability between parametric transducers is inherently so small as to be unmeasurable.

V. Conclusion

The transmission-phase relations have been written for four-frequency parametric transducers for various modes including the effects of varactor losses and cavity detuning. Four-frequency parametric transducers were considered because they encompass both the negative-conductance and frequency-conversion mechanisms of parametric amplification. These relations are also valid for the three- and two-frequency modes. At midband these relations reduce to simple, easily remembered equations which are valid for any type of nonlinear pumped circuit element.

The application of parametric transducers to monopulse systems because of their low-noise properties has been emphasized. There are other properties of parametric transducers that can be effectively applied to phase-sensitive systems. For example, if coherence between information channels is maintained by fulfilling the stated conditions, an array of radiators and parametric transducers may be scanned by appropriate phasing in the pump distribution.

A wideband differential phase bridge has been used to investigate the transmission phase properties of various parametric transducer modes. Midband transmission-phase relations have proved useful in the analysis of phase-sensitive instrumentation. The observed results vary in the manner predicted. The experimental results suggest that parametric transducers are ideally suited for phase-sensitive systems.